Microfluid Nanofluid (2011) 10:919–925
DOI 10.1007/s10404-010-0712-2

SHORT COMMUNICATION

Design and fabrication of microfluidic mixer from carbonyl iron–PDMS composite membrane

Jiaxing Li · Mengying Zhang · Limu Wang · Weihua Li · Ping Sheng · Weijia Wen

Received: 9 August 2010 / Accepted: 13 September 2010 / Published online: 12 October 2010

Abstract This paper introduces a carbonyl iron–PDMS (CI–PDMS) composite magnetic elastomer in which carbonyl iron (CI) particles are uniformly distributed in a PDMS matrix. The CI particles and the PDMS were mixed at different weight ratios and tested to determine the influence of CI concentration. The magnetic and mechanical properties of the magnetic elastomers were characterized, respectively, by vibrating-sample magnetometer and by tensile testing using a mechanical analyzer. The elastomer was found to exhibit high magnetization and good mechanical flexibility. The morphology and deformation of the CI–PDMS membrane also were observed. A magnetically actuated microfluidic mixer (that is, a micromixer) integrated with CI–PDMS elastomer membranes was successfully designed and fabricated. The high efficiency and quality of the mixing makes possible the impressive potential applications of this unique CI–PDMS material in microfluidic systems.

Keywords Magnetic elastomer · Membrane · Micromixer

1 Introduction

A lab-on-a-chip (LOC) is a device that integrates one or several laboratory functions on a single chip of only millimeters to a few square centimeters in size. A big boost in research and commercial interest came since mid 1990s. Microfluidics, which deals with the behavior, precise control, and manipulation of fluids that are geometrically constrained to a small, typically sub-millimeter, scale, is considered as an approbatory approach. To achieve multifunctions in microfluidic chips, especially sensors, actuators, and other active control components, various kinds of magnetic materials are employed. Permalloy and nickel thin films are widely used in MEMS devices (Khoo and Liu 2001; Myung et al. 2003; Gibbs et al. 2004; Li et al. 2009), whereas ferrofluid and magnetorheological (MR) fluid are applied to microfluidic systems in the designs of micro pumps and valves (Hatch et al. 2001; Hartshorne et al. 2004; Yamahata et al. 2005). Another important magnetic material in microfluidic systems is magnetic elastomer, which is a new type of composite consisting of small, usually nano- or micrometer-range magnetic particles dispersed in a highly elastic polymeric matrix. The combination of magnetic and elastic properties leads to a number of striking phenomena exhibited in response to magnetic fields (Abramchuk et al. 2007a, b; Fahrni et al. 2009b). Magnetic particles generally used are iron, nickel powder, Fe_3O_4, y-Fe_2O_3 magnetic powder and permalloy flaps, etc. (Khoo and Liu 2001; Abramchuk et al. 2007b; Martin et al. 2007; Peng et al. 2008; Pirmoradi et al. 2010). For the elastic polymeric matrix, silicone elastomer (Khoo and Liu 2001; Fahrni et al. 2009a), polyimide (Kohl et al. 1999), natural rubber (El-Nashar et al. 2006), and other materials are utilized.

The magnetic elastomer's merits, which include high elasticity, a remarkable deformational effect imparted by its low Young's modulus, a quick response to magnetic fields and potential actuation without on-chip power sources, have drawn much attention for the purposes of

J. Li · M. Zhang · L. Wang · P. Sheng · W. Wen (✉)
Department of Physics, KAUST-HKUST Joint Micro/Nano-Fluidic Laboratory, The Hong Kong University of Science and Technology, Clear Water Bay, Kowloon, Hong Kong
e-mail: phwen@ust.hk

W. Li
Faculty of Engineering, University of Wollongong, Wollongong, NSW 2522, Australia

magnetic elastomer membrane applications in micro valves, pumps, actuators (Khoo and Liu 2001; Wang et al. 2004; Fahrni et al. 2009a; Pirmoradi et al. 2010), and mixers (Huh et al. 2007). In fact, many researchers have investigated this novel material and its applications. For instance, Pirmoradi reported a new magnetic polymer membrane composed of coated iron oxide nanoparticles incorporated into a polydimethylsiloxane (PDMS) matrix (Pirmoradi et al. 2010), and Wang et al. (2004) presented results on the fabrication and testing of elastic permanent magnet films with microsize hard barium ferrite powder and different silicone elastomers. Most of these studies, however, have been handicapped by the disadvantages of low magnetization, small deflection or a complicated fabrication process. In this study, we introduced carbonyl iron (CI) of high saturated magnetization into a PDMS matrix, achieving a unique magnetic elastomer membrane that is responsive to low external magnetic field. This composite, easily fabricated, offers high magnetization and large deflection. As a means of demonstrating its remarkable properties and powerful applications in microfluidic systems, we designed and fabricated, based on our previous work (Niu et al. 2006a, b), a fast and effective micromixer.

2 Materials and methods

PDMS (Sylgard 184 Silicone Elastomer, Dow Corning Corporation), employed as the polymeric matrix, was acquired in the forms of two compounds, a pre-polymer and a cross-linker. CI powder (Fig. 1a) falling within the 4.8–5.2 μm diameter range was purchased from Sigma.

CI powder and PDMS pre-polymer were fully mixed for 20 min in a mortar and degassed in vacuum for 30 min (Fig. 1c), a process similar to that for Ag–PDMS (Niu et al. 2007). In the resultant CI–PDMS composites, the weight ratio of CI to PDMS ranged from 0.5 to 4.0.

The composites' morphology was visualized on a Philips SEM XL30 equipped for an acceleration voltage of 10 kV. The magnetization curves of the differing CI-to-PDMS ratio samples were measured by vibrating-sample magnetometer (VSM, LakeShore7037/9509-P). Their stress and strain behavior was measured by tensile testing using a mechanical analyzer (MTS Alliance RT/S). The specimens were fabricated in a custom, dog-bone-shaped mold having a width, thickness and length of 3.5 ± 0.1 mm, 1.8 ± 0.1 mm, and 6.3 ± 0.1 mm, respectively (Fig. 1d), and were baked in an oven at 65°C for 2 h. The temperature was held at 25°C over the entire testing period,

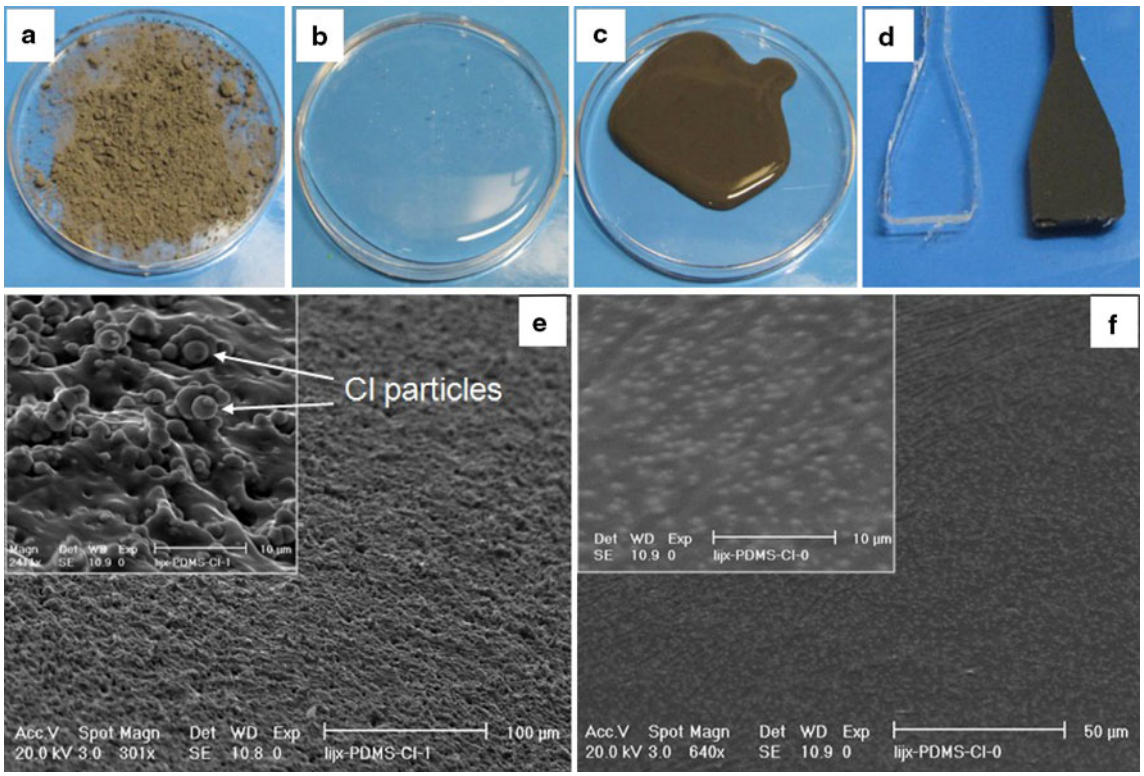

Fig. 1 Photographs of CI powders (**a**), liquid PDMS (**b**), liquid CI–PDMS composite (**c**), solid PDMS and CI–PDMS composite (**d**). SEM images of CI–PDMS composite (cross-section (**e**), and surface (**f**))

the applied loading was 0–25 N, and the applied speed was 3 cm/min.

The membrane deflection was measured as a function of the magnetic field, the source of which was an electromagnet. The magnetic field was characterized as a function of the distance from the magnet, using an F. W. Bell Gaussmeter. A microscope (Olympus 1X71, Olympus Imaging America Inc., PA, USA) and accessorial CCD were used to record and measured the deflection of membranes under different magnetic fields.

3 Results and discussion

Figure 1 shows SEM images of one of the CI–PDMS composites (weight ratio = 2). The SEM cross-section image (Fig. 1e) shows the micro CI particles dispersed in and affixed by the PDMS matrix. The distribution of the particles was quite uniform, and they were linked together by the PDMS without much aggregation. Figure 1f, an SEM image of the surface of the composite, exhibits uniformity, smoothness and a low surface roughness, qualities enabling easy bonding and good adhesion of membranes to substrates. The CI particles on the surface were not directly exposed to the air, thereby reducing the risk of particle oxidation and resulting surface roughness. These composite advantages improve membrane stability and facilitate chip fabrication.

Figure 2 shows the dependence of the magnetization on the magnetic fields applied to the different weight-ratio CI–PDMS composites at room temperature. The hysteresis loops of the magnetic CI particles distributed in the non-magnetic medium, PDMS, show clearly a soft magnetism behavior. The insert graph illustrates that with increasing CI/PDMS weight ratios, both the saturated magnetization (Ms) and the remnant magnetization (Mr) increased. However, it was very interesting to find that the coercivities (Hc) decreased with decreasing weight ratios. According to previous reports (e.g., El-Nashar et al. 2006), a larger ratio of magnetic particles in a rubber medium often shortens the distance between those particles, leading to magnetic coupling. In this study by contrast, due to the increased distance between the magnetic particles as caused by the low weight ratio, a weaker magnetic dipole coupling existed. Additionally, given the anti-ferromagnetic layer necessarily present on the surface of the CI particles due to the PDMS, this often led to some magnetic pole dead on their surface. The coercivities were found, correspondingly, to be non-linearly dependent on the CI/PDMS weight ratios in the composites. In the case of the aforementioned CI–PDMS composite (weight ratio = 2), the Ms was measured at 134.5 emu/g, which is much larger

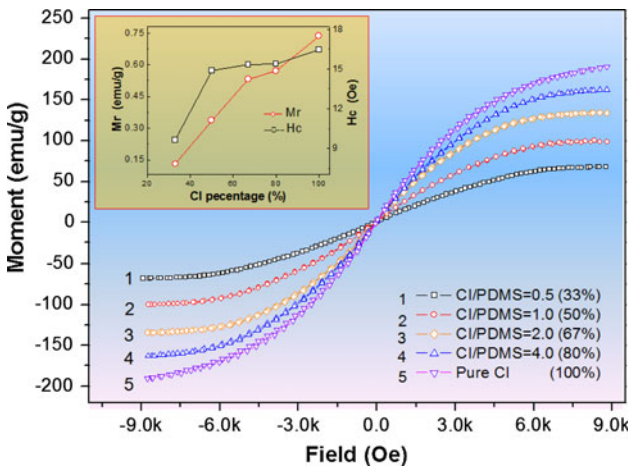

Fig. 2 Magnetization curves versus field strength for different CI–PDMS composites and pure CI powders. The *upper inset* graph shows the Mr, Hc of the different CI–PDMS composites and the pure CI powders

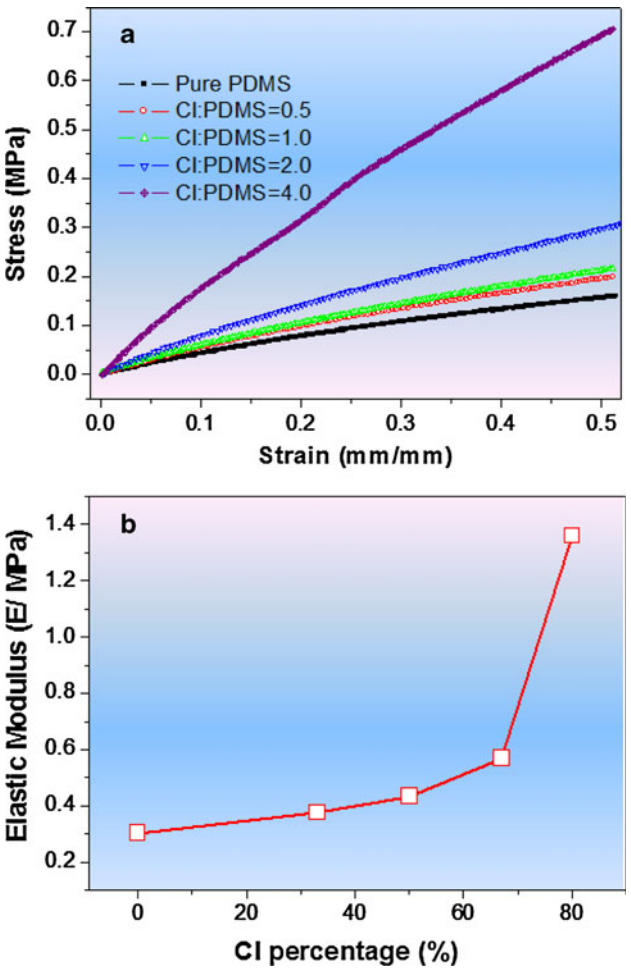

Fig. 3 Stress–strain curves (**a**) and elastic modulus (**b**) of pure PDMS and different CI–PDMS composites

than that of nickel particles–rubber composite, 25.03 emu/g (El-Nashar et al. 2006) or ferric oxide–PDMS composite, 21.9 emu/g (Pirmoradi et al. 2010). A large magnetization indicates that a large magnetic force can be exerted under a low magnetic field.

Figure 3 shows the stress–strain data of the pure PDMS and the CI–PDMS composites loaded with different CI/PDMS weight ratios. From Fig. 3a, it can be seen that in all of the cases, the curves are nearly linear. Each composite specimen was tested, and all showed an increase in Young's modulus compared with the pure PDMS, higher CI/PDMS ratios yielding more marked increases (Fig. 3b). The surface characteristics of the filler material determine the chemical and physical interaction between the filler and the polymer chain network, and in that way greatly affect the mechanical properties of the composites. The reduction in the Young's modulus of a polymer composite, then, could be the result of poor interactions between the filler material and the polymer network (Bokobza and Rapoport 2002; Pirmoradi et al. 2010). Accordingly, the increased Young's modulus of the CI–PDMS composites indicates that the interaction between the CI particles and the polymer network was quite strong. The base and curing agent weight ratio has a large effect on the modulus value of regular PDMS (Armani et al. 1999). The ratio we applied here was 15:1 for the magnetic membrane, and its Young's modulus was tested at 0.31 E/MPa. The low Young's modulus is advantageous, since a large deflection can be achieved with lower magnetic fields.

The deformation of the magnetic elastomer membrane was investigated, and some of the results are shown in Fig. 4. An electromagnetic magnet was positioned above each free-standing magnetic CI–PDMS composite membrane of 1.0 ± 0.05 mm diameter and 100 ± 5 μm thickness. As Fig. 4a indicates, the membrane deflection increased as the CI content increased from ratio = 0.5 to ratio = 2, but it decreased from ratio = 2 to ratio = 4. To understand this phenomenon, we should compare the Young's modulus (Fig. 3b) and the magnetization (Fig. 2) at the different ratios. From ratio = 0.5 to ratio = 2, the magnetization doubled, but the Young's modulus increased only by about 30%; in other words, the force increased greatly but the magnetostriction did not, resulting in the overall effect, being the increased deformation of the membrane. However, comparing the situations with ratio = 2 and ratio = 4, we found that the magnetization rose by about 20% whereas the Young's modulus almost doubled, which overall should effect a drop in the deformation. From the above analysis, we could conclude that, for a magnetically actuated mixer, the optimized membrane CI/PDMS ratio is around 2. We used this ratio to further test the membrane deformation under different magnetic field strengths. Figure 4b clearly illustrates that the membrane deflection increased with the increasing magnetic field.

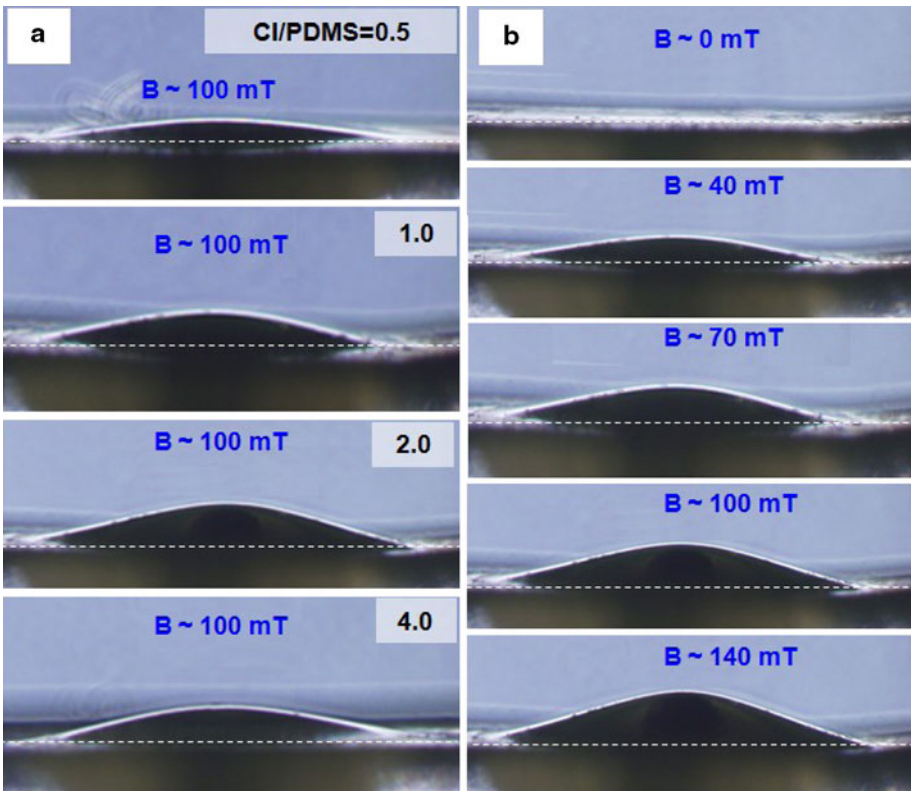

Fig. 4 Deflection of different CI–PDMS elastomer membranes (~1.0 mm in diameter, ~100 μm in thickness) under same magnetic field (**a**). Membrane (ratio = 2) deflection as function of magnet field (**b**)

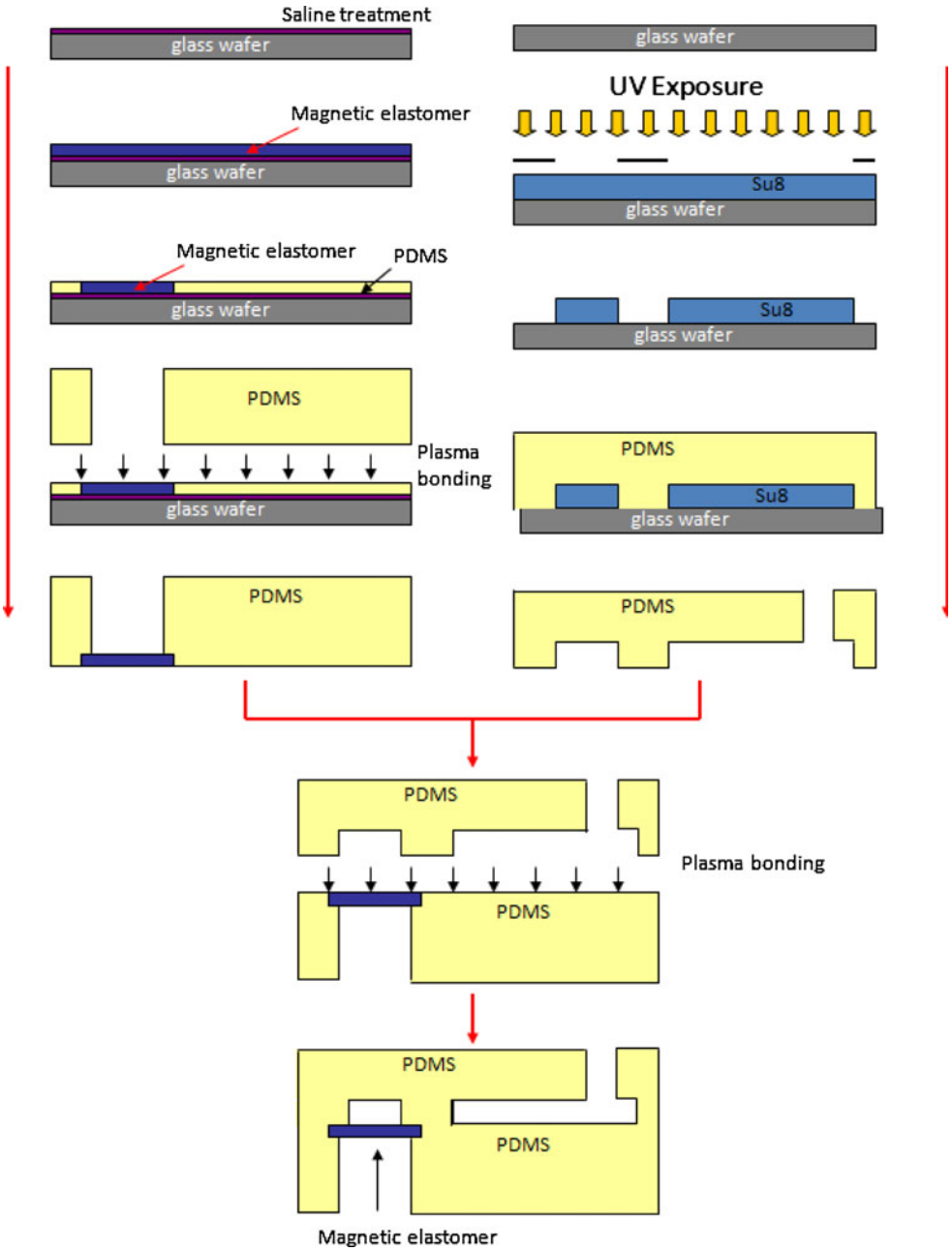

Fig. 5 Fabrication process for micromixer chip

Those unique properties of this CI–PDMS magnetic composite show that it is possible to achieve membrane actuation in various applications such as valves, pumps, and micromixers.

4 Magnetically actuated microfluidic mixer

Mixing two or more steams of laminar flows in microfluidic is an important issue for lab-on-a-chip devices. Passive geometries were designed to generate perturbation, and active control was introduced to achieve chaotic mixing. In active mixer design, side channels were incorporated to connect to a chamber of a membrane actuated by external force. A gas valve (Unger et al. 2000), an electrically controlled mechanical valve (Thorsen et al. 2002) and electrorheological (ER) fluid (Niu et al. 2006a, b) were used to trigger and control the movement of the membrane to generate chaotic mixing in a microfluidic system. Some magnetically actuated micromixers in microfluidics were reported recently (Biswal and Gast 2004; Li et al. 2005; Ryu et al. 2004; Suzuki et al. 2004; Wen et al. 2009). Our micromixer was designed and fabricated to incorporate the many advantages of the novel CI–PDMS magnetic membrane already discussed here.

Figure 5 illustrates the fabrication process for our micromixer chip consisting of three PDMS layers with the

CI–PDMS magnetic membrane embedded in the middle layer. The mold for the channel layer was formed by standard photolithography using negative photoresist SU8-2025 on a glass wafer. The channel layer and supporting layer were fabricated of PDMS (base: curing agent = 10:1). CI–PDMS pre-polymer, consisting of CI particles and PDMS mixture (base: curing agent = 15:1) at the weight ratio of 2, was spin-coated on a PMMA plate and solidified in an oven to produce a thin film of about 100 μm thickness. Then, pieces were cut to proper size and placed at certain positions on a silanized (trichloro 1*H*, 1*H*,2*H*,2*H*-perfluorooctyl silane, ALDRICH) glass wafer. PDMS pre-polymer (base: curing agent = 15:1) was then spin-coated on the same glass wafer to form a thin layer of ~100 μm uniform thickness. This thin layer was then aligned with the channel layer and supporting layer, adhesion being achieved by oxygen plasma bonding. A microfluidic chip of sandwich structure thereby was derived, a schematic view of which, along with an optical overhead photo, are shown in Fig. 6a and b. In Fig. 6a, the microfluidic channel (pink) is about 40 μm in height and 200 μm in width; the chambers and the holes in the sides of the magnetic membrane are about 1 mm in diameter, and the holes in the supporting layer were formed to allow space for membrane deformation. While a magnetic field is applied, the CI–PDMS elastomer membrane deforms and pushes or pulls the fluid into the chambers. Because the chambers are connected to the main channel by side channels, the flow in the main channel incurs some disturbance.

In order to demonstrate the mixing effect, we pumped two streams of dyed DI water (blue and red) at a flow rate of about 0.1 ml/h and actuated the membrane by 10 Hz square-wave-sharped magnetic field (DC current, the field strength varies between 0 and 100 mT). As Fig. 6c makes clear, without the magnetic field, the two water streams had a clear interface owing to the dominance of the viscous effect in the micro channel. Once the magnetic field was applied, mixing occurred where the side channels meet the main channel. Resultantly, the interface disappeared as the water color became uniform, reflecting the uniform mixing between the two streams.

5 Conclusions

This paper explicated the fabrication process and application of CI–PDMS magnetic composites formed of CI particles embedded in a PDMS matrix. Experiments demonstrated the composites' high magnetization, good flexibility and stability. From this unique material, a large deflection magnetic membrane could be designed and fabricated, the optimized CI/PDMS weight ratio of which was found to be 2. Additionally, a realistic micromixer application incorporating this CI–PDMS magnetic membrane was successfully demonstrated. Indeed, the results obtained are very promising for a variety of microfluidic device applications, especially active fluid control.

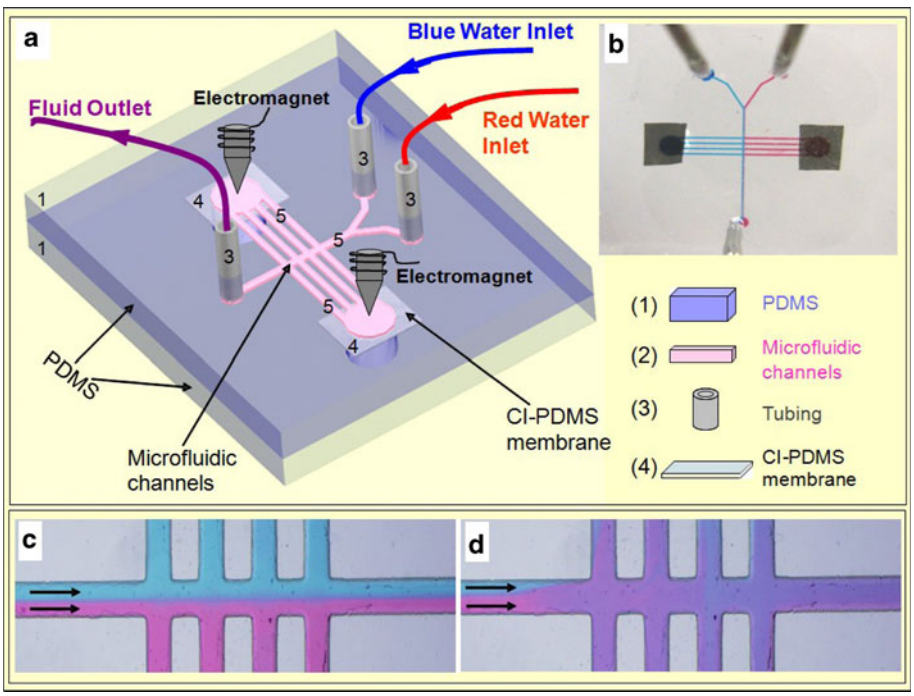

Fig. 6 Schematic illustration showing magnetically actuated mixer design and construction (**a**). Photographic image of mixer chip (**b**). Optical photo of channel without perturbation (**c**), channel after full mixing (**d**)

Acknowledgments This publication is based on work partially supported by Award No. SA-C0040/UK-C0016, made by King Abdullah University of Science and Technology (KAUST), Hong Kong RGC grants HKUST 603608. The work was also partially supported by the Nanoscience and Nanotechnology Program at HKUST. The authors would like to give thanks to Dr. Yongjian Wang and Dr. Zuli Xu for their help in the SEM image taking.

References

Abramchuk S, Kramarenko E, Grishin D, Stepanov G, Nikitin LV, Filipcsei G, Khokhlov AR, Zrinyi M (2007a) Novel highly elastic magnetic materials for dampers and seals: part II. Material behavior in a magnetic field. Polym Adv Technol 18:513–518

Abramchuk S, Kramarenko E, Stepanov G, Nikitin LV, Filipcsei G, Khokhlov AR, Zrinyi M (2007b) Novel highly elastic magnetic materials for dampers and seals: part I. Preparation and characterization of the elastic materials. Polym Adv Technol 18:883–890

Armani D, Liu C, Alum N (1999) Re-configurable fluid circuits by PDMS elastomer micromachining. MEMS'99. Twelfth IEEE international conference, pp 222–227

Biswal SL, Gast AP (2004) Micromixing with linked chains of paramagnetic particles. Anal Chem 76:6448–6455

Bokobza L, Rapoport O (2002) Reinforcement of natural rubber. J Appl Polym Sci 85:2301–2316

El-Nashar DE, Mansour SH, Girgis E (2006) Nickel and iron nanoparticles in natural rubber composites. J Mater Sci 41:5359–5364

Fahrni F, Prins MWJ, van IJzendoorn LJ (2009a) Magnetization and actuation of polymeric microstructures with magnetic nanoparticles for application in microfluidics. J Magn Magn Mater 321:1843–1850

Fahrni F, Prins MWJ, van Ijzendoorn LJ (2009b) Micro-fluidic actuation using magnetic artificial cilia. Lab Chip 9:3413–3421

Gibbs MRJ, Hill EW, Wright PJ (2004) Magnetic materials for MEMS applications. J Phys D Appl Phys 37:R237–R244

Hartshorne H, Backhouse CJ, Lee WE (2004) Ferrofluid-based microchip pump and valve. Sensor Actuator B Chem 99: 592–600

Hatch A, Kamholz AE, Holman G, Yager P, Bohringer KF (2001) A ferrofluidic magnetic micropump. J Microelecthomech Syst 10:215–221

Huh YS, Choi JH, Park TJ, Hong YK, Hong WH, Lee SY (2007) Microfluidic cell disruption system employing a magnetically actuated diaphragm. Electrophoresis 28:4748–4757

Khoo M, Liu C (2001) Micro magnetic silicone elastomer membrane actuator. Sensor Actuator A Phys 89:259–266

Kohl M, Skrobanek KD, Miyazaki S (1999) Development of stress-optimised shape memory microvalves. Sensor Actuator A Phys 72:243–250

Li CW, Wang YN, Gao YH, Guo XY, Gu ZZ (2005) Magnetically actuated micromixing on an array-pattern microfluidic chip for immunoassay of human thyrotropin. J Nanosci Nanotechnol 5:1297–1300

Li XW, Jia X, Xie CL, Lin Y, Cao R, He QZ, Chen P, Wang XC, Liang SP (2009) Development of cationic colloidal silica-coated magnetic nanospheres for highly selective and rapid enrichment of plasma membrane fractions for proteomics analysis. Biotechnol Appl Biochem 54:213–220

Martin M, Hanagud S, Thadhani NN (2007) Mechanical behavior of nickel plus aluminum powder-reinforced epoxy composites. Mater Sci Eng A Struct 443:209–218

Myung NV, Park DY, Yoo BY, Sumodjo PTA (2003) Development of electroplated magnetic materials for MEMS. J Magn Magn Mater 265:189–198

Niu XZ, Liu LY, Wen WJ, Sheng P (2006a) Active microfluidic mixer chip. Appl Phys Lett 88:153508

Niu XZ, Liu LY, Wen WJ, Sheng P (2006b) Hybrid approach to high-frequency microfluidic mixing. Phys Rev Lett 97:044501

Niu XZ, Peng SL, Liu LY, Wen WJ, Sheng P (2007) Characterizing and patterning of PDMS-based conducting composites. Adv Mater 19:2682–2686

Peng SL, Zhang MY, Niu XZ, Wen WJ, Liu ZY, Shi J, Sheng P (2008) Magnetically responsive elastic microspheres. Appl Phys Lett 92:012108

Pirmoradi F, Cheng LN, Chiao M (2010) A magnetic poly(dimethylesiloxane) composite membrane incorporated with uniformly dispersed, coated iron oxide nanoparticles. J Micromech Microeng 20:015032

Ryu KS, Shaikh K, Goluch E, Fan ZF, Liu C (2004) Micro magnetic stir-bar mixer integrated with parylene microfluidic channels. Lab Chip 4:608–613

Suzuki H, Ho CM, Kasagi N (2004) A chaotic mixer for magnetic bead-based micro cell sorter. J Microelectromech Syst 13:779–790

Thorsen T, Maerkl SJ, Quake SR (2002) Microfluidic large-scale integration. Science 298:580–584

Unger MA, Chou HP, Thorsen T, Scherer A, Quake SR (2000) Monolithic microfabricated valves and pumps by multilayer soft lithography. Science 288:113–116

Wang WS, Yao ZM, Chen JC, Fang J (2004) Composite elastic magnet films with hard magnetic feature. J Micromech Microeng 14:1321–1327

Wen CY, Yeh CP, Tsai CH, Fu LM (2009) Rapid magnetic microfluidic mixer utilizing AC electromagnetic field. Electrophoresis 30:4179–4186

Yamahata C, Chastellain M, Parashar VK, Petri A, Hofmann H, Gijs MAM (2005) Plastic micropump with ferrofluidic actuation. J Microelecthomech Syst 14:96–102